A DNA-based three-state device

Bernard Yurke
Bell Laboratories
Lucent Technologies
Murray Hill, NJ 07974

Friedrich C. Simmel*
Bell Laboratories,
Lucent Technologies
Murray Hill, NJ 07974

Abstract

A simple DNA-based nanomechanical device is presented which can be switched between three different conformations by the addition of appropriate signal molecules. Two of these conformations are mechanically rigid. The device consists of two arms formed by double-stranded DNA, connected by a single-stranded hinge. The device can be in a closed or stretched configuration, and in an intermediate relaxed state. The operation of the device is monitored by fluorescence resonance energy transfer and gel electrophoresis experiments. The closing of the supramolecular arms is affected by the salt concentration, probably due to electrostatic interactions of the device with itself.

1 INTRODUCTION

Its molecular recognition properties make DNA a promising molecule for the development of molecular nanotechnology. DNA has already been utilized to build a number of complex nanoscale structures [1, 2, 3]. Moreover, in recent experiments the remarkable properties of DNA could even be used to induce motion on a molecular scale [4, 5, 6, 7, 8, 9, 10]. The basis for molecular engineering with DNA is the – under appropriate conditions – highly specific base pair (bp) recognition between the DNA bases adenine (A) and thymine (T), and between guanine (G) and cytosine (C) [11]. By the choice of base sequence, DNA strands can be made "sticky" or non-interacting. The "programmability" of these interactions renders DNA particularly interesting as a self-assembly molecule as it offers much more design freedom than available in other self-assembly approaches [12]. In the case of nanomechanical devices, the information-carrying character of DNA is not only utilized for the assembly of the devices but also as a means of addressing (and therefore controlling) their conformational transitions. Here we present a simple DNA-based device which can be switched between three different mechanical states. Starting from a relaxed intermediate conformation, the device can either be transferred to a stretched or to a tightened state, depending on the "fuel" or "signal" strand added to it. From these configurations the device can be returned to the original state, and therefore this simple molecular machine can be controllably cycled through its different states. Earlier DNA constructs like DNA tweezers [5], DNA actuator [6, 8] or DNA scissors [7] based upon the same operation principle were switchable only between a flexible and a rigid conformation. A combination of tweezers and actuator resulted in a three-state device (TSD) which could be switched between two rigid and one flexible state [10]. In the present work, we provide additional evidence for the proper operation of this TSD. We also investigate the influence of ionic strength on the different conformations of the device and thereby demonstrate the flexibility of the relaxed state as opposed to the rigidness of the stretched and the tightened state.

2 DESCRIPTION OF THE DEVICE

The three-state device in its relaxed conformation is assembled from the 40 nucleotide (nt) long DNA strand Q and the 84 nt long strand R (Fig. 1). Q and R form two 18 bp long "arms," connected by 4 nt and 48 nt long single-stranded sections. The ≈ 13.6 nm long arms are mechanically stiff elements on this length scale, as they are considerably shorter than the persistence length of double-stranded DNA (about 50 nm [13]). The single-stranded sections, however, are rather flexible [14]. During the device's operation the 4 nt section acts as a hinge, whereas the long 48 nt section is used to address and induce the motion of the

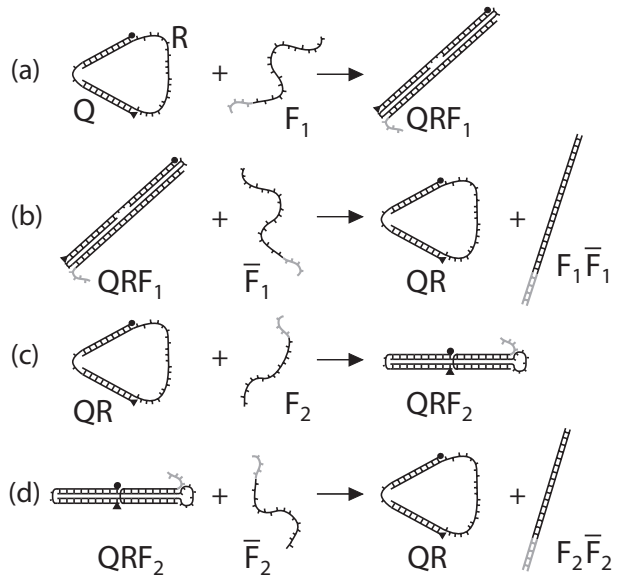

Figure 1: Schematic representation of the operation principle of the three-state device: (a) The TSD consists of two single strands of DNA, Q and R. They hybridize together to form two double-stranded arms connected by a hinge and a long single-stranded section. The TSD is stretched by the fuel strand F_1 which hybridizes to the single-stranded part of QR. (b) The removal strand $\bar{F}_1$ can attach to an unhybridized section of F_1 (depicted in gray) and remove F_1. This restores the relaxed conformation. (c) F_2 can hybridize with QR in a different manner and thus close the arms of the device. (d) Similar to (b) the relaxed state can be restored by the addition of $\bar{F}_2$.

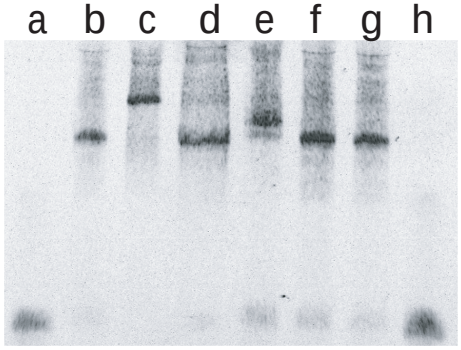

Figure 2: Fluorescence image of the result of a 10% polyacrylamide gel electrophoresis run of the TSD and its components. DNA strands run from the top to the bottom of the gel; smaller complexes run faster. Lanes (a) and (h) contain strand Q, lanes (b) and (g) the relaxed TSD (Q + R). Lane (c) contains the stretched TSD (QR + F_1). In lane (d) the fuel strand has been removed again (QRF$_1$ + $\bar{F}_1$). In lane (e) the TSD is in its closed conformation (QR + F_2). The band shift is smaller than in lane (c) as F_2 is shorter than F_1. Finally, in (f) the closing strand has been removed to restore the relaxed state of the TSD (QRF$_2$ + $\bar{F}_2$). Only complexes containing the fluorescently labeled strand Q are visible in this image. The smears above the main bands are caused by multimerization products. Several Q strands can be linked together by R strands and several QR complexes can be crosslinked by fuel strands. This effect has been extensively discussed in Refs. [5, 6, 8]

TSD.

The conformational transitions of the TSD are depicted in Fig. 1: The relaxed device (QR) can be transferred into the stretched configuration (QRF$_1$) with the help of the 48 nt long fuel strand F_1 (Fig. 1 (a)). As F_1 hybridizes with the long single-stranded section of QR, the formation of the DNA duplex straightens the TSD. In Fig. 1 (b) the TSD is returned to its relaxed state. F_1 is equipped with a short eight base long section (drawn in gray) which does not hybridize to QR. At this overhang section F_1 can be attacked by $\bar{F}_1$ which is a strand complementary to F_1. The fuel strand F_1 is removed from QRF$_1$ by $\bar{F}_1$ in a process known as "branch migration" [15]. In this process, both QR and $\bar{F}_1$ compete for binding to F_1. During branch migration, the branch point, at which the three strands R, F_1 and $\bar{F}_1$ meet, performs a random walk along R. When the branch point makes its first passage, the strand displacement process is completed and the "inert" waste product $F_1\bar{F}_1$ falls off the now relaxed TSD.

The tightening (or closing) motion of the TSD is shown in Fig. 1 (c). Here, a different 40 nt long fuel strand F_2 is used which hybridizes to R in a manner reverse to that of the straightening transition. F_2 pulls the two arms of the device close together. A short ring-like section of R is left unhybridized to facilitate the attack of the second removal strand $\bar{F}_2$ which again restores the relaxed configuration by branch migration (Fig. 1 (d)). Using the appropriate fuel and removal strands, the TSD can be switched arbitrarily between its three conformations QR, QRF$_1$, and QRF$_2$.

3 METHODS

Oligonucleotides were synthesized, labeled and purified by Integrated DNA Technologies, Inc. (IDT). The sequences for the strands can be found in references [6, 10]. The operation of the TSD is checked

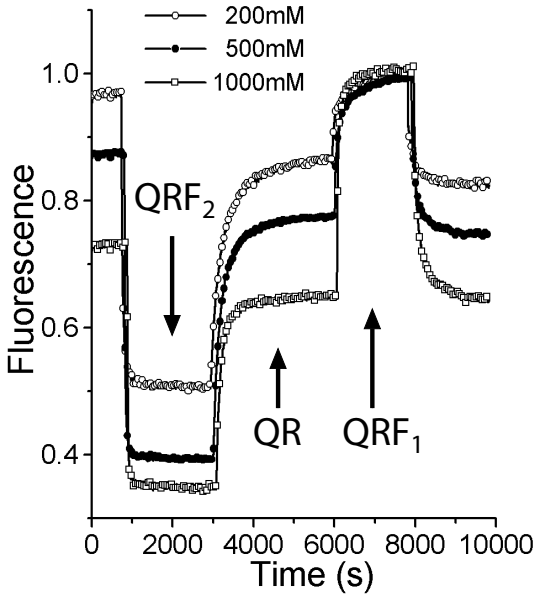

Figure 3: The TSD operation is monitored with fluorescence measurements at three different salt concentrations: The devices start in the relaxed configuration (QR). By the addition of fuel strand F_2 they are transferred into the closed conformation (QRF_2). From there, they are returned to state QR with the removal strand $\bar{F}_2$. Subsequently, the TSD is brought into the stretched state QRF_1 by the addition of fuel strand F_1. Removal of this strand with its complement $\bar{F}_1$ completes one operation cycle. The changes in the fluorescence levels are due to FRET and correspond to changes in the separation between the fluorescent dyes attached to the arm of the TSD (see Fig. 1).

with gel electrophoresis and fluorescence resonance energy transfer experiments. For the latter, strand Q is labeled at the 5' end with the fluorescent dye TET (2',4',5',7'-Tetrachloro-5(6)-carboxyfluorescein) and at the 3' end with TAMRA (N,N,N',N'-Tetramethyl-5(6)-carboxyrhodamine) (symbolized by the black circles and triangles in Fig. 1). TET and TAMRA form a fluorescence resonance energy transfer (FRET) pair [16] with a Förster distance R_0 of approximately 5 nm. The emission band of TET (the "donor") and the absorption band of TAMRA (the "acceptor") overlap and TET can transfer its excitation energy nonradiatively to TAMRA. This quenches the TET fluorescence. The energy transfer efficiency depends strongly on the distance between donor and acceptor. At a distance R_0 between the dyes, the efficiency of energy transfer is 50%. To estimate dye separations, we use an experimentally obtained calibration curve [5, 17]. For the FRET experiments, the relaxed devices are assembled by mixing stoichiometric amounts of 25 μM solutions of strands Q and R in TE buffer (10 mM Tris(hydroxymethyl)-aminomethane (Tris), pH 8.0, 1 mM ethylene diamine tetraacetic acid (EDTA)) and diluting these mixtures in reaction buffer to a final concentration of 1 μM. As reaction buffers we used TE buffer with added salt (TE/200 mM NaCl, TE/500 mM NaCl, TE/1M NaCl) or "physiological buffer" (potassium phosphate buffer, pH 7.2, with $[K^+]$=140 mM, $[Na^+]$=10 mM and $[Mg^{2+}]$=0.5 mM (intracellular values) [18]). The TSDs are switched between their different conformations by the addition of stoichiometric amounts of 25 μM fuel or removal strands, followed by rapid mixing. The fluorescence of TET is excited with light from an Argon ion laser (λ = 514.5 nm) chopped at a frequency of 130 Hz. The fluorescence light is filtered with a 10 nm bandpass filter centered at 540 nm and detected with a Si photodiode at the chopper frequency.

For the gel electrophoresis experiments, strands are mixed in stoichiometric amounts at a concentration of 2.5μM in TE buffer. Polyacrylamide gels were cast at a concentration of 10% and run at 10 V/cm and $T = 20°$C. To visualize the bands, the gels were illuminated using the laser system described above and photographed through a bandpass filter with a digital camera.

4 RESULTS

In Fig. 2 the result of a gel run in a 10% polyacrylamide gel is displayed. The band shifts correspond to the molecular weight changes of the TSD during its operation. Lanes (a) and (h) contain only strand Q, whereas lanes (b) and (g) contain the relaxed conformation QR. In the remaining lanes the TSD is cycled once through its states: Straightened (lane c), relaxed (lane d), closed (lane e) and relaxed again (lane f). The band shifts visible on the gel image correspond to the increase or decrease of the molecular weight of the TSD with the attachment or removal of fuel strands.

Typical FRET signals collected during the operation of the TSD are shown in Fig. 3 for three different salt concentrations. The fluorescence of the device in its straightened conformation (QRF_1) has been normalized to one, as this conformation is least influenced by the salt concentration. In the straightened conformation, the sample displays its maximum fluorescence, as in this state the two dyes are furthest apart from each

other and therefore FRET is least efficient. In the intermediate state (QR), TET and TAMRA are closer to each other, and therefore the fluorescence is partly quenched. This effect is stronger for higher salt concentrations. In the closed state QRF_2, the two dyes are brought very close to each other, and therefore the TET fluorescence is quenched most efficiently. In this conformation, the fluorescence of the device is also lower for higher salt concentrations. However, its sensitivity is not as strong as for the relaxed state. The transitions between the conformations display second order kinetics with reaction half-times on the order of $t_{1/2} = 10$ s – 100 s. The reactions are generally faster for higher salt concentrations [19].

For possible biomedical applications it is important to investigate whether nanomechanical devices as the TSD are operable under physiological conditions. To this end, a wide range of salt concentrations, pH values and temperatures have been investigated. It is found that the temperature dependence of the reaction kinetics exhibits the expected Arrhenius-like behavior. The fluorescence signal changes are highest for high (monovalent) ion concentrations and low temperatures, whereas they are relatively insensitive to changes in the pH value [19]. For Fig. 4, the TSD has been operated in physiological buffer at $T = 37$°C. The half-times for completion of the reactions are comparable to the ones for the data presented above: The lower salt concentrations slow the reactions down, whereas the higher temperature speeds them up. The changes in the fluorescence intensity are considerably less under physiological conditions than at lower temperatures and higher salt concentrations.

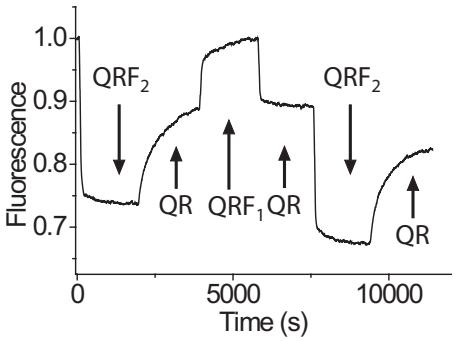

Figure 4: The TSD is also operable under physiological conditions (physiological buffer at $T = 37$°C). Under these conditions the reaction kinetics and the fluorescence signal levels are altered. Higher temperature speeds up the reactions; the lower salt concentrations have the opposite effect. Also, the fluorescence intensity changes decrease with higher temperature.

5 DISCUSSION

The gel electrophoresis band shifts in Fig. 2 and the fluorescence changes in Fig. 3 are in full agreement with the proposed operation scheme for the TSD from Fig. 1. From the fluorescence levels one can deduce the distances between the dyes for the different conformations at different salt concentrations. In the stretched state their separation is 13.6 nm which is just the length of a 40 bp double helix. In the relaxed state the separations between the dyes are 8.2 nm, 6.2 nm and 5.1 nm for sodium ion concentrations of 200 mM, 500 mM and 1 M, respectively. In the closed state the corresponding separations are approximately 3.7 nm, 2.7 nm and 2.0 nm. This shows that at high salt concentrations the device can be switched between two rigid conformations which is a major improvement over earlier devices based on the same operation principle [5, 6]. These devices could only be switched between one rigid and one flexible conformation. The

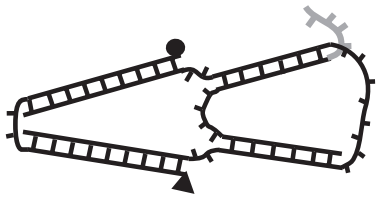

Figure 5: Model of closed TSD at low salt concentration. Reduced screening leads to mutual electrostatic repulsion of the arms. This partly unzips the fuel strand F_2 from R.

flexibility of the relaxed configuration would severely constrain the performance of the two-state devices if operated against an externally applied force. With the three-state device and its two rigid conformations this limitation is overcome. It can be expected that the TSD is capable of actually performing work against an external force if it is switched between the tightened and stretched configurations. However, our results indicate that at low salt concentrations the closed state of the TSD also becomes distorted. Due to the reduced screening of electrostatic interactions at low ion concentrations, the arms of the device begin to push on each other and the distance between the arms increases. This explains the increase of the fluorescence intensity in the closed state for low salt concentrations. At low enough salt concentrations, the mutual repulsion becomes strong enough to break base pairs (Fig. 5). A quantitative treatment of this effect might provide a possibility to calibrate the forces generated by the TSD. In the relaxed state, the reduced screening at lower salt concentrations probably results in the

stiffening of the single-stranded section of strand R which also pushes the dyes further apart.

The TSD is an example of a chemically addressable molecular device. The fuel strands F_1 and F_2 can be thought of as signal strands with which one can externally control the conformational changes of the device. Based on this principle, more elaborate molecular devices could be developed which are capable of a larger number of conformational changes controllable in a similar fashion as the TSD. Alternatively, a population of devices could be devised, which are capable of interacting with each other with the help of signal strands. A possible application of this might lie in the assembly of nanoscale components in a certain spatiotemporal order, e.g., the installation of molecular electronic components. Interacting DNA devices might also be used to construct chemical reaction networks performing particular tasks. It has to be mentioned that the construction of complex machines or networks faces similar problems as DNA-based computation: The number of machines (or conformations, interactions, etc.) is limited by the number of distinct base sequences available which robustly assemble into the correct structures without unwanted cross-hybridizations. Otherwise, incorrectly assembled devices, extensive crosslinking and high error rates in addressing the devices will make an operation of the machines impracticable.

Apart from nanotechnology and molecular electronics, possible applications of DNA nanodevices can also be found in the biomedical area. Molecular devices could be used as drug delivery systems or biosensors. With results obtained in the field of DNA-based computing, one could even combine the mechanical operation of the devices with information processing activities. The stable operation of our DNA devices under physiological conditions makes such a biomedical application quite plausible, even though for such an application the usual problems of gene delivery would have to be solved first.

6 CONCLUSIONS

We have demonstrated the construction and operation of a DNA-based molecular device which is switchable between three different conformations. Two of these conformations are mechanically robust. Due to the highly charged nature of DNA, the device operation is strongly affected by changes in the salt concentration of the reaction buffer. However, the device is still operable under physiological conditions.

Acknowledgments

Financial support by the Alexander von Humboldt Foundation through the Feodor Lynen program is gratefully acknowledged (F.C.S).

*present address: Center for NanoScience and Sektion Physik, Ludwig-Maximilians-Universität, Geschwister-Scholl-Platz 1, 80539 München, Germany.

References

[1] J. Chen and N. C. Seeman, Nature **350**, 631 (1991).

[2] C. Mao, W. Sun, and N. C. Seeman, Nature **386**, 137 (1997).

[3] E. Winfree, F. Liu, L. A. Wenzler, and N. C. Seeman, Nature **394**, 539 (1998).

[4] C. Mao, W. Sun, Z. Shen, and N. C. Seeman, Nature **397**, 144 (1999).

[5] B. Yurke, A. J. Turberfield, A. P. Mills Jr., F. C. Simmel, and J. L. Neumann, Nature **406**, 605 (2000).

[6] F. C. Simmel and B. Yurke, Phys. Rev. E **63**, 041913 (2001).

[7] J. C. Mitchell and B. Yurke, DNA 7, Seventh International Meeting on DNA-Based Computers, Springer Lecture Notes in Computer Science, in print (2002).

[8] F. C. Simmel and B. Yurke, DNA 7, Seventh International Meeting on DNA-Based Computers, Springer Lecture Notes in Computer Science, in print (2002).

[9] H. Yan, X. Zhang, Z. Shen, and N. C. Seeman, Nature **415**, 62 (2002).

[10] F. C. Simmel and B. Yurke, Applied Physics Letters **80**, 883 (2002).

[11] V. A. Bloomfield, D. M. Crothers, and I. Tinoco Jr., *Nucleic Acids*, University Science Books, Sausalito (2000).

[12] J. J. Storhoff and C. A. Mirkin, Chem. Rev. **99**, 1849-1862 (1999).

[13] S. B. Smith, Y. Cui, and C. Bustamante, Science **271**, 795 (1996).

[14] B. Tinland, A. Pluen, J. Sturm, and G. Weill, Macromolecules **30**, 5763 (1997).

[15] I. G. Panyutin and P. Hsieh, Proc. Natl. Acad. Sci. USA **91**, 2021 (1994).

[16] L. Stryer and R. P. Haugland, Proc. Nat. Acad. Sci. USA **58**, 719 (1967).

[17] F. C. Simmel and B. Yurke, Proc. SPIE **4332**, 419 (2001).

[18] B. Alberts, D. Bray, J. Lewis, M. Raff, K. Roberts and J. D. Watson, *Molecular Biology of the Cell*, 3rd ed., Garland Publishing, New York (1994).

[19] F. C. Simmel, B. Yurke, and R. J. Sanyal, submitted to J. Nanosc. Nanotech. (2002).